Supplementary Tables and Figures

Record	Region	Latitude	Longitude	Proxy	Sampling distance (yr)	Reference	Data source
Lake Chichancanab	Mexico	19°05'N	88°45'W	$\delta^{18}O$	20, 20, 21	29	1
Cariaco Basin	Gulf of Cariaco	10°42'N	65°01'W	Ti conc.	5.4, 5.5, 5.8	30	2
GISP2	Greenland	72°35'N	38°28'W	$\delta^{18}O$	9.7,12.3,16.2	26	3
GRIP	Greenland	72°35'N	37°38'W	$\delta^{18}O$	20, 20, 20	24	4
NGRIP	Greenland	75°06'N	42°18'W	$\delta^{18}O$	20, 20, 20	27	4
Agassiz Ice Cap	N. Canada	80°49'N	72°56'W	$\delta^{18}O$	25, 25, 25	28	5
Renland	Greenland	71°15'N	26°46'W	$\delta^{18}O$	20, 20, 20	25	4
MD99-2275	Iceland shelf	66°33'N	17°42'W	Alkenones	4.8, 4.8, 5.1	50	6

Supplementary Table S1. Overview of the climate-proxy records. The three numbers in the sampling distance column denote the 25%, 50% (median), and 75% percentiles (i.e. ¼ of the sampling distances are smaller than the first number in the column, whereas ¼ are larger than the last number in the column). In the table, we cite the original data sources for all the Arctic ice cores, but for the following ice cores NGRIP, GRIP, and Renland, we have used the data series that have been compiled and transferred to the GICC05 time scale[27]. All the records included in the table fulfil the selection criteria mentioned below, except for core MD99-2275 (blue colour). For this reason, the record from core MD99-2275 is only included as part of the supplementary material, where it is used for comparison purposes.

Data sources:

1: ftp://ftp.ncdc.noaa.gov/pub/data/paleo/paleolimnology/yucatan/chichancanab.txt
2: ftp://ftp.ncdc.noaa.gov/pub/data/paleo/paleocean/sediment_files/complete/odp1002h-fwc.txt
3: ftp://ftp.ncdc.noaa.gov/pub/data/paleo/icecore/greenland/summit/gisp2/isotopes/gispd18o.txt
4: http://www.iceandclimate.nbi.ku.dk/data/
5: ftp://ftp.ncdc.noaa.gov/pub/data/paleo/icecore/polar/agassiz/a77del18_25yr.txt
6: Personal communication with the author

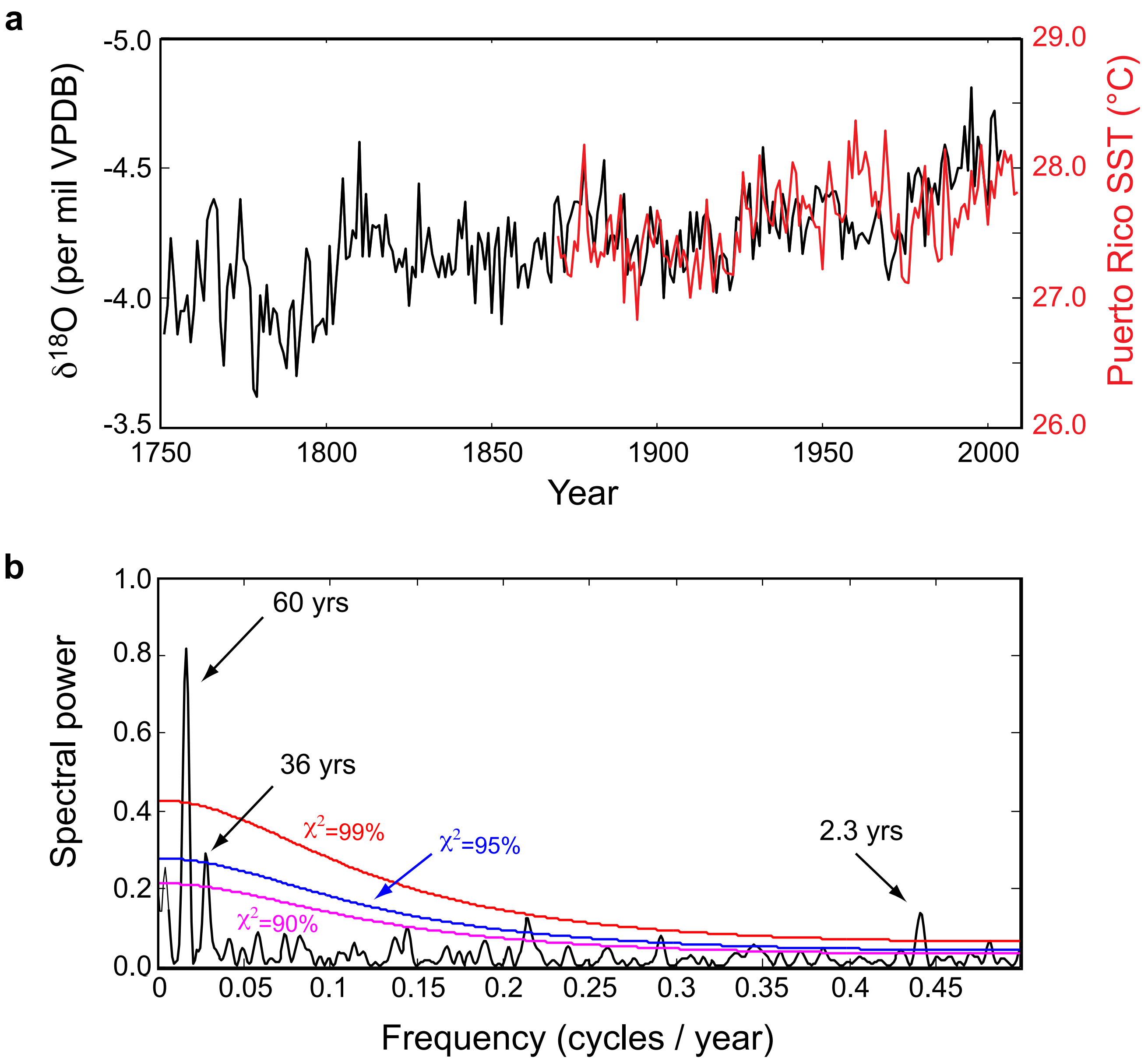

Supplementary Figure S1. Caribbean sea-surface temperature reconstruction based on coral $\delta^{18}O$ from southwestern Puerto Rico. (a) Coral $\delta^{18}O$ data from Puerto Rico[14] (black curve), which have been used to reconstruct sea-surface temperatures (SST) in the Caribbean over the past ~250 years. The red curve shows the annual mean SST just south of Puerto Rico (data from HADISST[58]) (**b**) Power spectrum associated with he coral $\delta^{18}O$ data from Puerto Rico. The power spectrum in **b** was constructed by use of the Lomb-Scargle Fourier transform and the red-noise false-alarm levels (pink, blue, and red lines) were calculated using the publicly available program REDFIT 3.8[31]. This approach yields results that are identical to those obtained by Kilbourne et al., (2008), who used a completely different method (Multitaper Method). Note that a 60-yr oscillation appears to be by far the most dominant oscillation in Caribbean SST over the past 250 years.

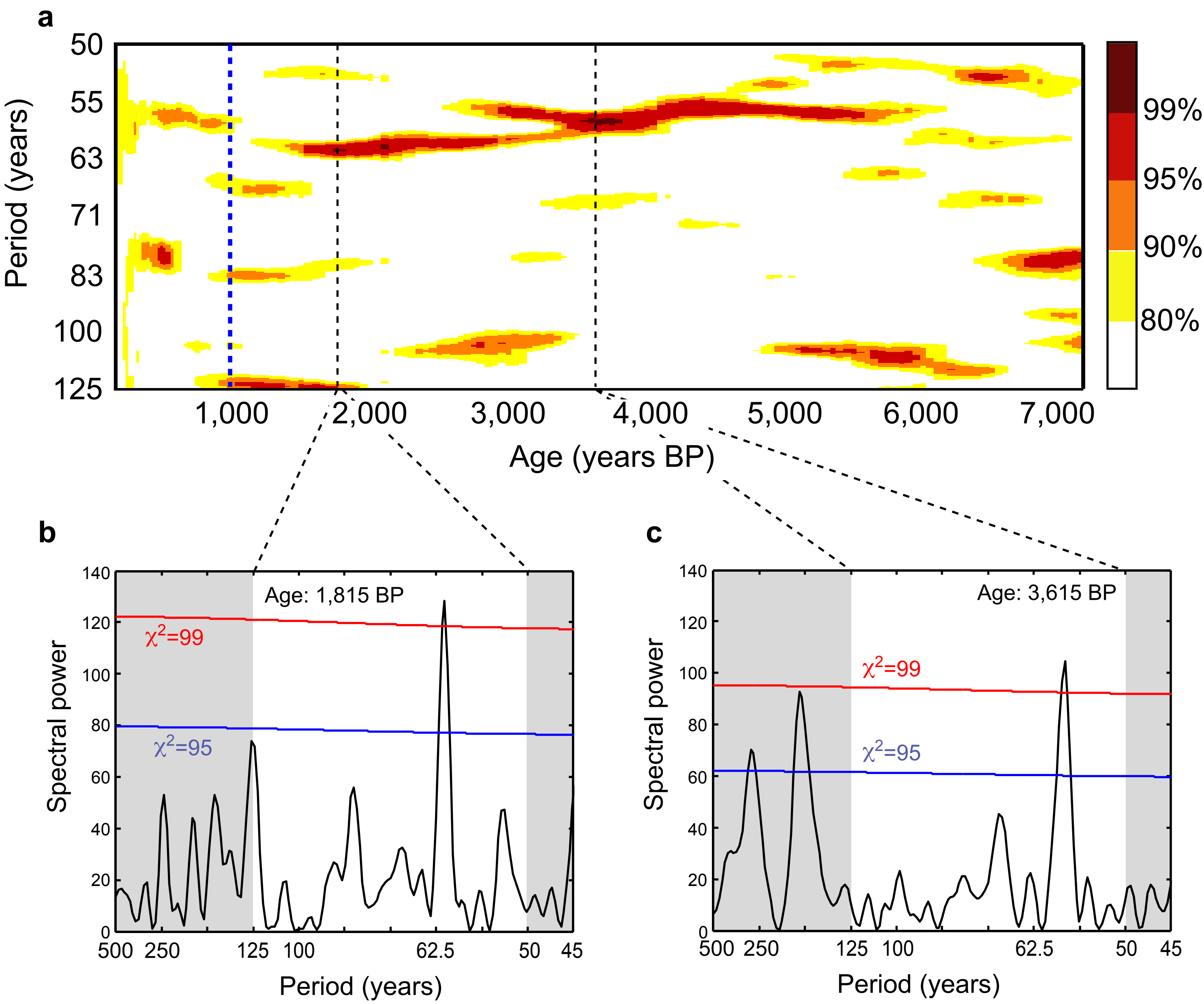

Supplementary Figure S2. Spectral density distribution of the δ^{18}O record from Lake Chichancanab[29], Mexico. (**a**) Temporal distribution of spectral power that exceeds the red-noise false-alarm levels. The colour coding indicates that the spectral power exceeds the 80%, 90%, 95%, and 99% false-alarm levels, respectively. The spectrogram delineating the statistically significant spectral power is calculated using the Lomb-Scargle fourier transform[53,54] on data grouped in 2,000-yr windows, with a spacing of 50 years between each window. However, for the interval covering the last 1,000 years (left of the dashed blue line), the size of the time window was linearly decreased from 2,000 years to 200 years in steps of 25 years. (**b**) An example of the spectral power distribution calculated for a 2,000-yr data window centered at 1,815 BP, and (**c**) the spectral power distribution of a 2,000-yr window centered at 3,615 BP. The white zones in **b** and **c** indicate the frequency interval used to construct the spectrogram in **a**. The blue and red lines in **b** and **c** denote the 95% and 99% red-noise false-alarm levels, respectively, which were calculated using the publicly available program REDFIT 3.8[31]. Notice the dominance of the spectral peaks around 60 years in **b** and **c.**

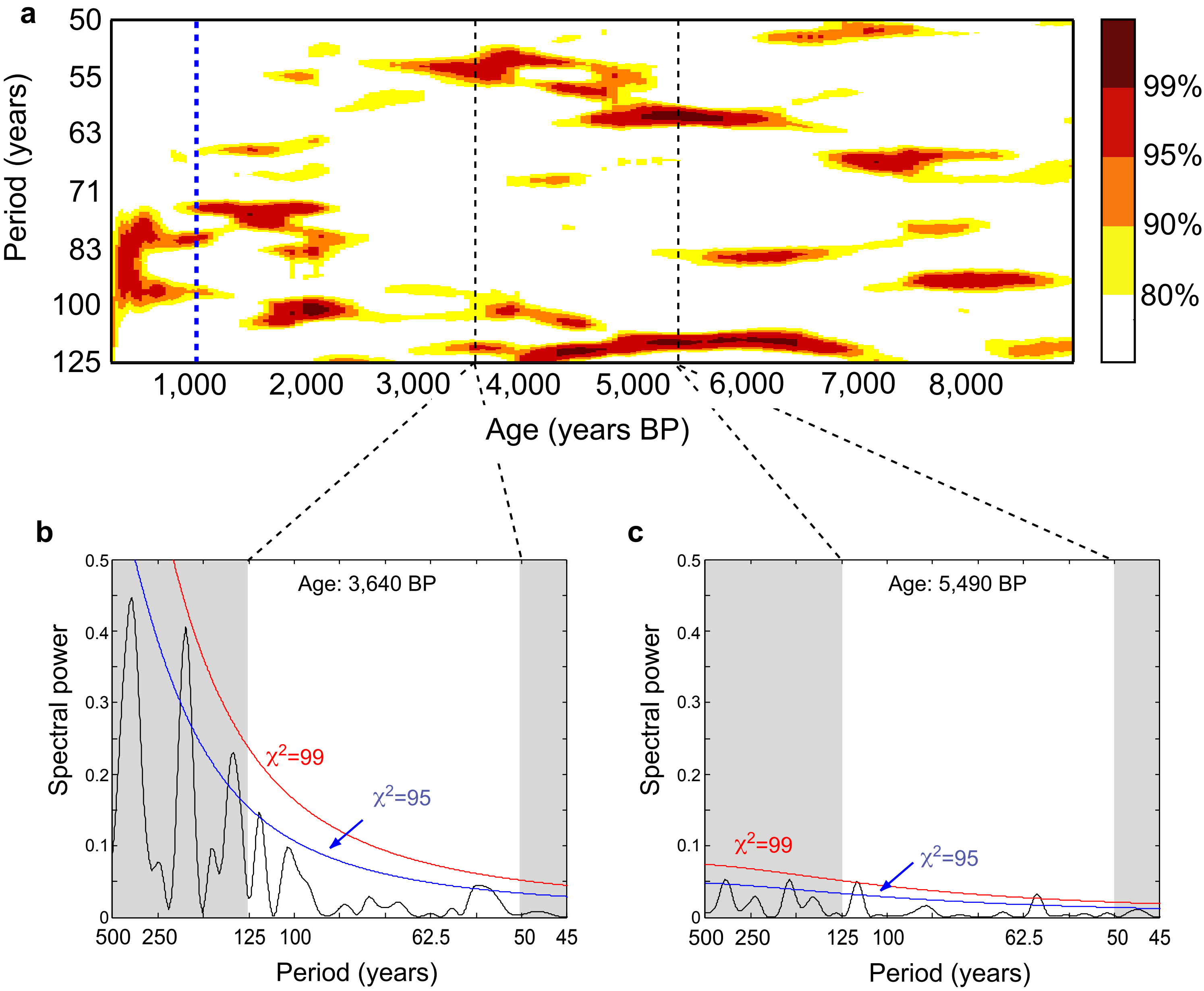

Supplementary Figure S3. Spectral density distribution of the Ti (%) record from the Cariaco Basin[30] north of Venezuela. (**a**) Temporal distribution of spectral power that exceeds the red-noise false-alarm levels. The colour coding indicates that the spectral power exceeds the 80%, 90%, 95%, and 99% false-alarm levels, respectively. The spectrogram delineating the statistically significant spectral power is calculated using the Lomb-Scargle fourier transform[53,54] on data grouped in 2,000-yr windows, with a spacing of 50 years between each window. However, for the interval covering the last 1,000 years (left of the dashed blue line), the size of the time window was linearly decreased from 2,000 years to 200 years in steps of 25 years. (**b**) An example of the spectral power distribution calculated for a 2,000-yr data window centered at 3,640 BP, and (**c**) the spectral power distribution of a 2,000-yr window centered at 5,490 BP. The white zones in **b** and **c** indicate the frequency interval used to construct the spectrogram in **a**. The blue and red lines in **b** and **c** denote the 95% and 99% red-noise false-alarm levels, respectively, which were calculated using the publicly available program REDFIT 3.8[31]. For the densely sampled raw data (~6 per yr) the periods shorter than ~20 yr had spectral amplitudes, which did not fit the AR1 model. We brought this record on a more equal footing with the other datasets by resampling the densely sampled raw data to double sample distance (12 yr), yielding two new “half-records”. The resulting spectral periods of the two “half-records”, now down to 24 yr, did fit an AR1 process adequately for our analysis to proceed. We then calculated all spectra associated with the two new “half-records” in order to finally average the spectra and false-alarm levels associated with each time window. This approach ensured that all the data were used, and that the data complied with the red-noise model. Spectral peaks around ~60 years are found to be statistically significant (99% level) in the Ti record from the Cariaco Basin, but, contrary to the other climate records included in this study, these peaks do not represent the dominant spectral peaks of this record.

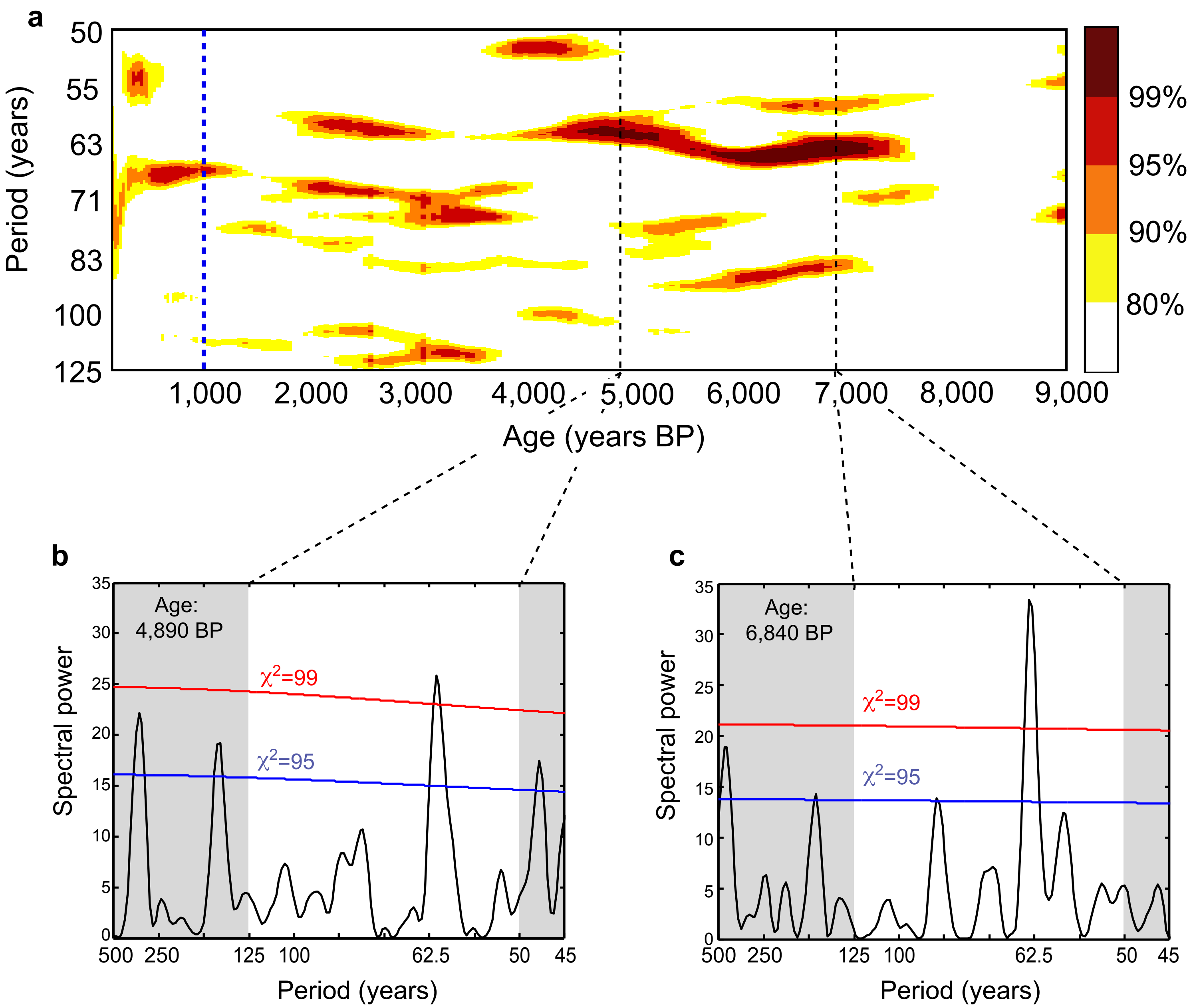

Supplementary Figure S4. Spectral density distribution of the δ^{18}O record from the GISP2 ice core[26], Greenland. (**a**) Temporal distribution of spectral power that exceeds the red-noise false-alarm levels. The colour coding indicates that the spectral power exceeds the 80%, 90%, 95%, and 99% false-alarm levels, respectively. The spectrogram delineating the statistically significant spectral power is calculated using the Lomb-Scargle fourier transform[53,54] on data grouped in 2,000-yr windows, with a spacing of 50 years between each window. However, for the interval covering the last 1,000 years (left of the dashed blue line), the size of the time window was linearly decreased from 2,000 years to 200 years in steps of 25 years. (**b**) An example of the spectral power distribution calculated for a 2,000-yr data window centered at 4,890 BP, and (**c**) the spectral power distribution of a 2,000-yr window centered at 6,840 BP. The white zones in **b** and **c** indicate the frequency interval used to construct the spectrogram in **a**. The blue and red lines in **b** and **c** denote the 95% and 99% red-noise false-alarm levels, respectively, which were calculated using the publicly available program REDFIT 3.8[31]. Notice the dominance of the spectral peaks around 62-65 years in **b** and **c.**

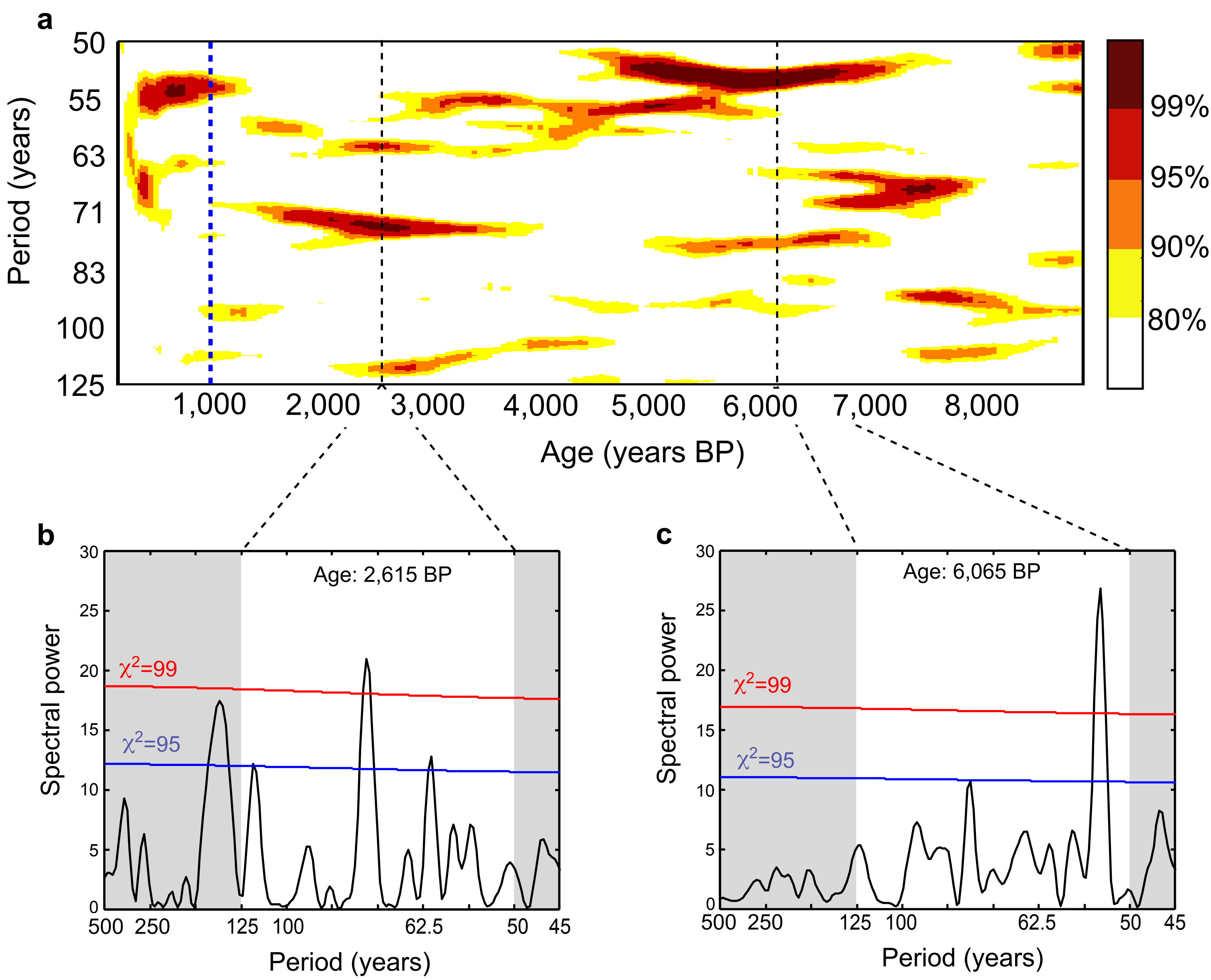

Supplementary Figure S5. Spectral density distribution of the δ^{18}O record from the GRIP ice core[24], Greenland. (**a**) Temporal distribution of spectral power that exceeds the red-noise false-alarm levels. The colour coding indicates that the spectral power exceeds the 80%, 90%, 95%, and 99% false-alarm levels, respectively. The spectrogram delineating the statistically significant spectral power is calculated using the Lomb-Scargle fourier transform[53,54] on data grouped in 2,000-yr windows, with a spacing of 50 years between each window. However, for the interval covering the last 1,000 years (left of the dashed blue line), the size of the time window was linearly decreased from 2,000 years to 200 years in steps of 25 years. (**b**) An example of the spectral power distribution calculated for a 2,000-yr data window centered at 2,615 BP, and (**c**) the spectral power distribution of a 2,000-yr window centered at 6,065 BP. The white zones in **b** and **c** indicate the frequency interval used to construct the spectrogram in **a**. The blue and red lines in **b** and **c** denote the 95% and 99% red-noise false-alarm levels, respectively, which were calculated using the publicly available program REDFIT 3.8[31]. Notice the dominance of the spectral peak around 54 years in **c.** The spectrogram in **a** is based on the new GRIP record that is tied to the GICC05 time scale[27], which has a temporal resolution of 20 years. A similar result is, however, obtained if we use the GRIP record tied to the ss09 time scale[31], which has an average temporal resolution of ~4 years.

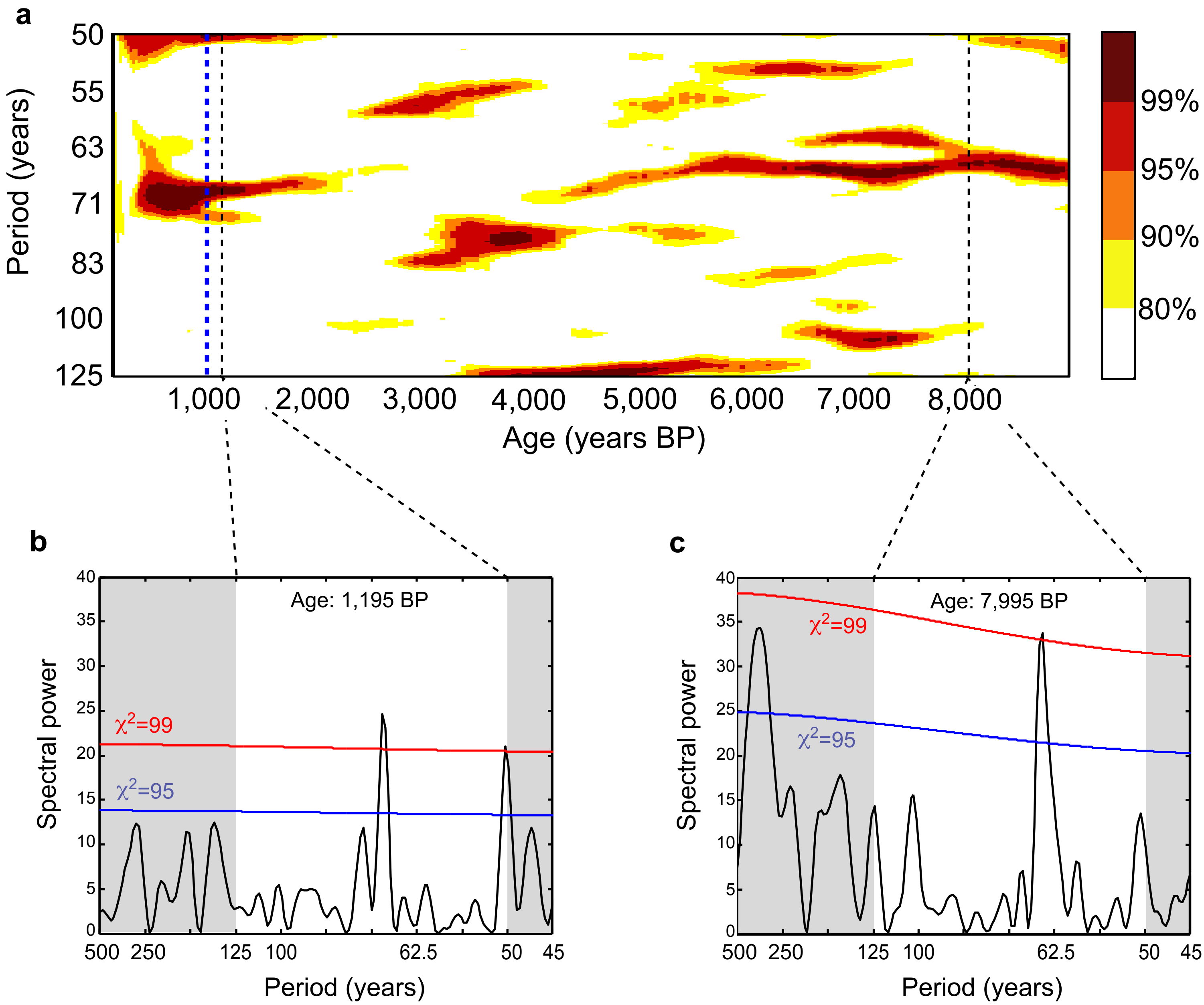

Supplementary Figure S6. Spectral density distribution of the $\delta^{18}O$ record from the NGRIP ice core[27], Greenland. (**a**) Temporal distribution of spectral power that exceeds the red-noise false-alarm levels. The colour coding indicates that the spectral power exceeds the 80%, 90%, 95%, and 99% false-alarm levels, respectively. The spectrogram delineating the statistically significant spectral power is calculated using the Lomb-Scargle fourier transform[53,54] on data grouped in 2,000-yr windows, with a spacing of 50 years between each window. However, for the interval covering the last 1,000 years (left of the dashed blue line), the size of the time window was linearly decreased from 2,000 years to 200 years in steps of 25 years. (**b**) An example of the spectral power distribution calculated for a 2,000-yr data window centered at 1,195 BP, and (**c**) the spectral power distribution of a 2,000-yr window centered at 7,995 BP. The white zones in **b** and **c** indicate the frequency interval used to construct the spectrogram in **a**. The blue and red lines in **b** and **c** denote the 95% and 99% red-noise false-alarm levels, respectively, which were calculated using the publicly available program REDFIT 3.8[31]. Notice the dominance of the spectral peaks around ~65 years in **b** and **c.**

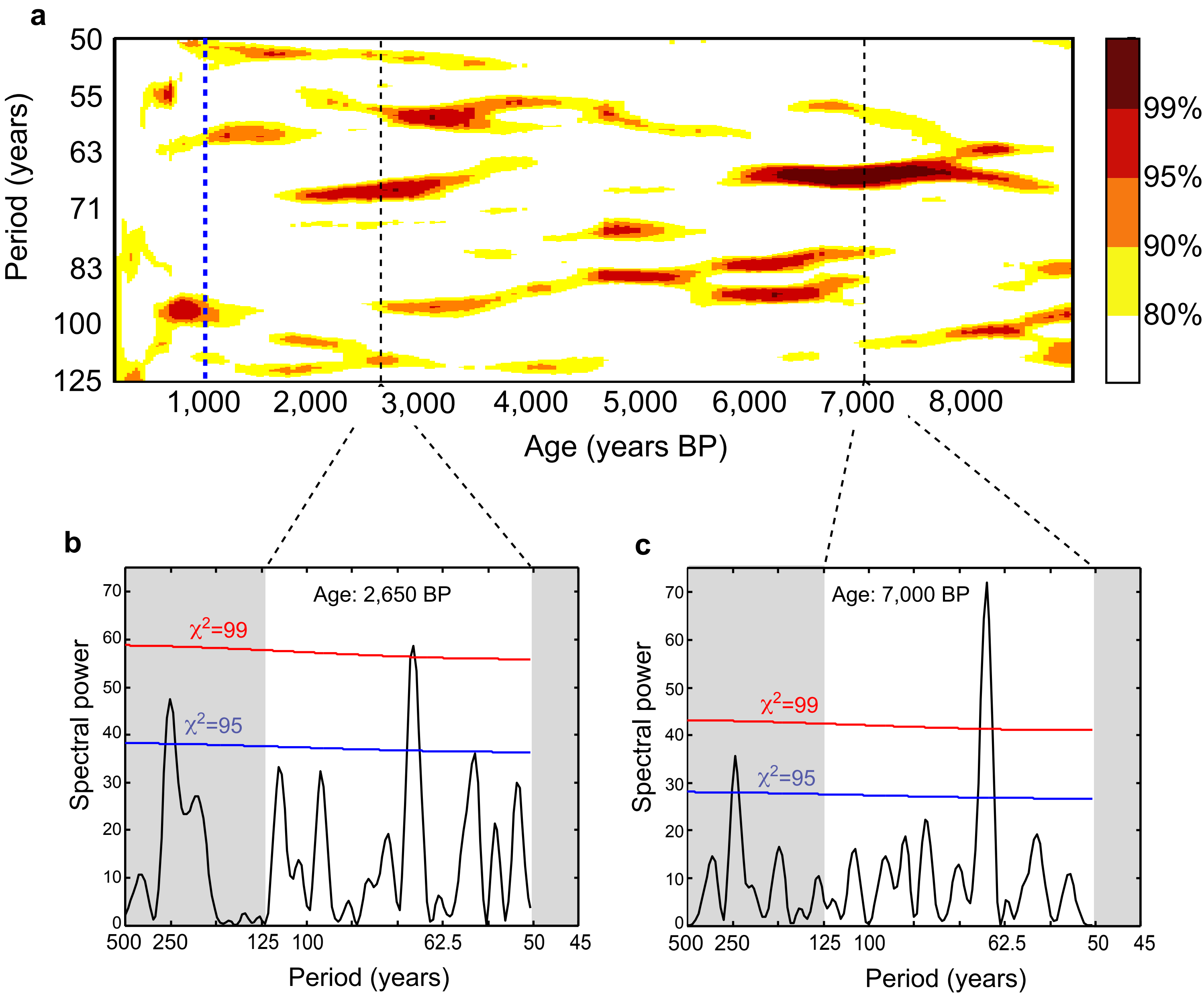

Supplementary Figure S7. Spectral density distribution of the $\delta^{18}O$ record from the Agassiz ice cap[28], Canada. (**a**) Temporal distribution of spectral power that exceeds the red-noise false-alarm levels. The colour coding indicates that the spectral power exceeds the 80%, 90%, 95%, and 99% false-alarm levels, respectively. The spectrogram delineating the statistically significant spectral power is calculated using the Lomb-Scargle fourier transform[53,54] on data grouped in 2,000-yr windows, with a spacing of 50 years between each window. However, for the interval covering the last 1,000 years (left of the dashed blue line), the size of the time window was linearly decreased from 2,000 years to 200 years in steps of 25 years. (**b**) An example of the spectral power distribution calculated for a 2,000-yr data window centered at 2,650 BP, and (**c**) the spectral power distribution of a 2,000-yr window centered at 7,000 BP. The white zones in **b** and **c** indicate the frequency interval used to construct the spectrogram in **a**. The blue and red lines in **b** and **c** denote the 95% and 99% red-noise false-alarm levels, respectively, which were calculated using the publicly available program REDFIT 3.8[31]. Notice the dominance of the spectral peak around ~64 years in panel **c.**

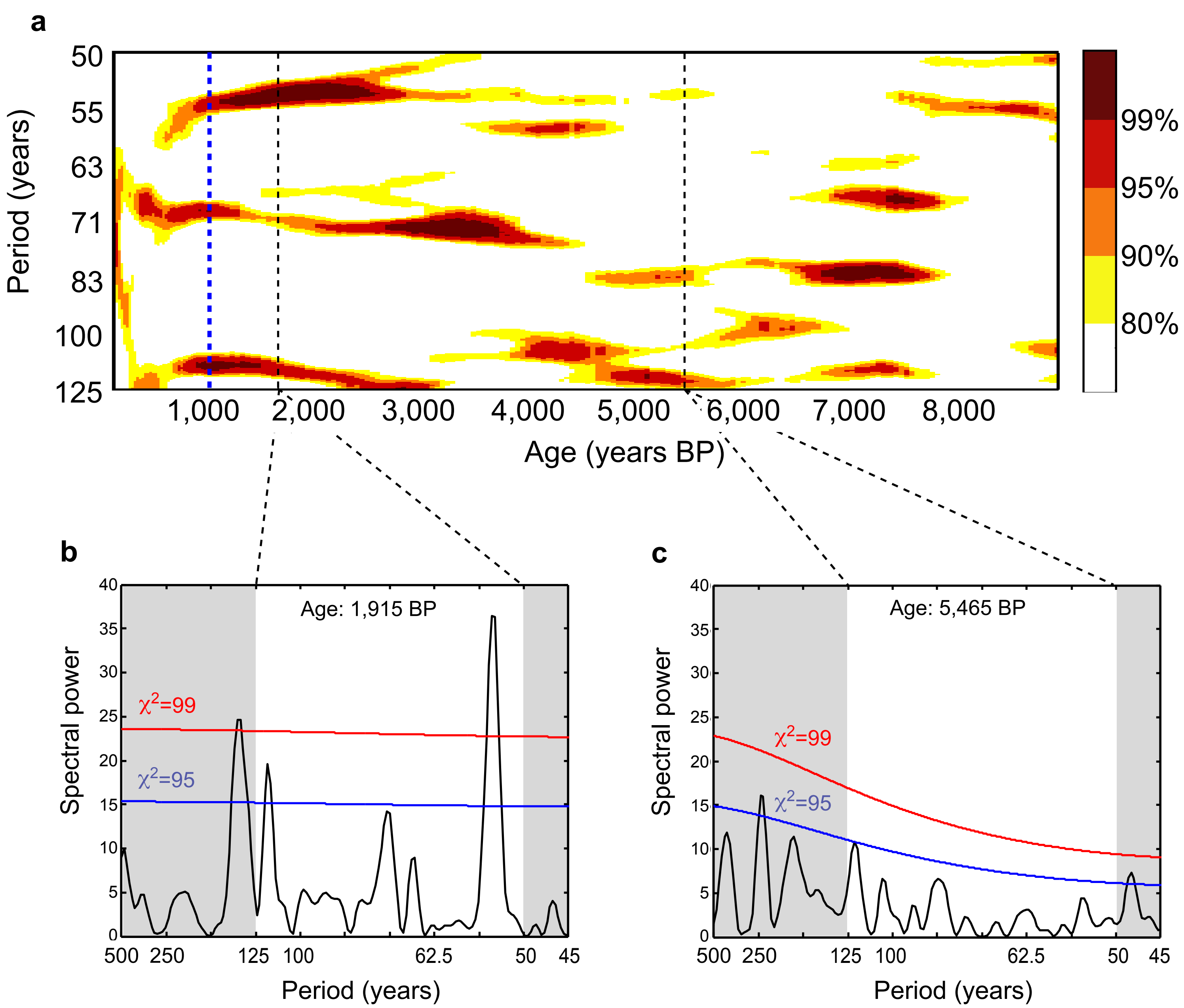

Supplementary Figure S8. Spectral density distribution of the δ^{18}O **record from the Renland ice core[25], Greenland**. (**a**) Temporal distribution of spectral power that exceeds the red-noise false-alarm levels. The colour coding indicates that the spectral power exceeds the 80%, 90%, 95%, and 99% false-alarm levels, respectively. The spectrogram delineating the statistically significant spectral power is calculated using the Lomb-Scargle fourier transform[53,54] on data grouped in 2,000-yr windows, with a spacing of 50 years between each window. However, for the interval covering the last 1,000 years (left of the dashed blue line), the size of the time window was linearly decreased from 2,000 years to 200 years in steps of 25 years. (**b**) An example of the spectral power distribution calculated for a 2,000-yr data window centered at 1,915 BP, and (**c**) the spectral power distribution of a 2,000-yr window centered at 5,465 BP. The white zones in **b** and **c** indicate the frequency interval used to construct the spectrogram in **a**. The blue and red lines in **b** and **c** denote the 95% and 99% red-noise false-alarm levels, respectively, which were calculated using the publicly available program REDFIT 3.8[31]. Notice the dominance of the spectral peak around ~54 years in **b.**

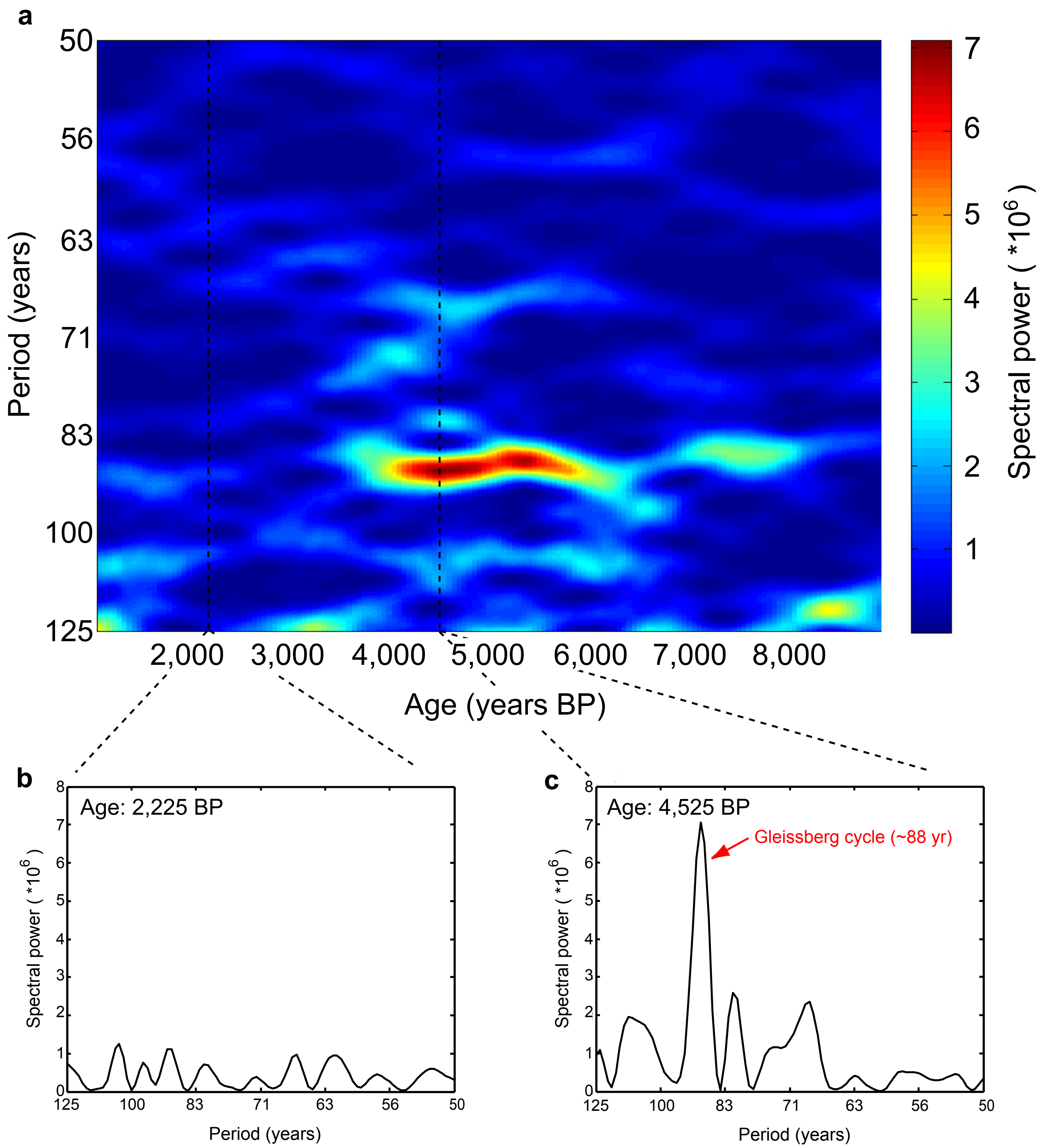

Supplementary Figure S9. Spectral density distribution of solar reconstruction based on ^{14}C from the radiocarbon calibration curve[32]. (**a**) Spectrogram calculated using the Lomb-Scargle fourier transform[53,54] on data grouped in 2000-yr windows, with a spacing of 50 years between each window. Note that similar spectral density distribution is obtained if the regular Fourier transform is used instead of the Lomb-Scargle fourier transform. For the solar spectrogram based on ^{14}C, we show the distribution of spectral power, and not the spectral power exceeding the false-alarm levels, so the differences between the spectral power of various frequencies (periods) can be assessed. Moreover, other studies have already established which solar cycles are statistically significant. (**b**) An example of the spectral power distribution calculated for a 2,000-yr data window centered at 2,225 BP, and (**c**) the spectral power distribution of a 2,000-yr window centered at 4,525 BP. Notice that the Gleissberg cycle (~88 yr) is by far the most dominant feature in this frequency range of the ^{14}C spectrum.

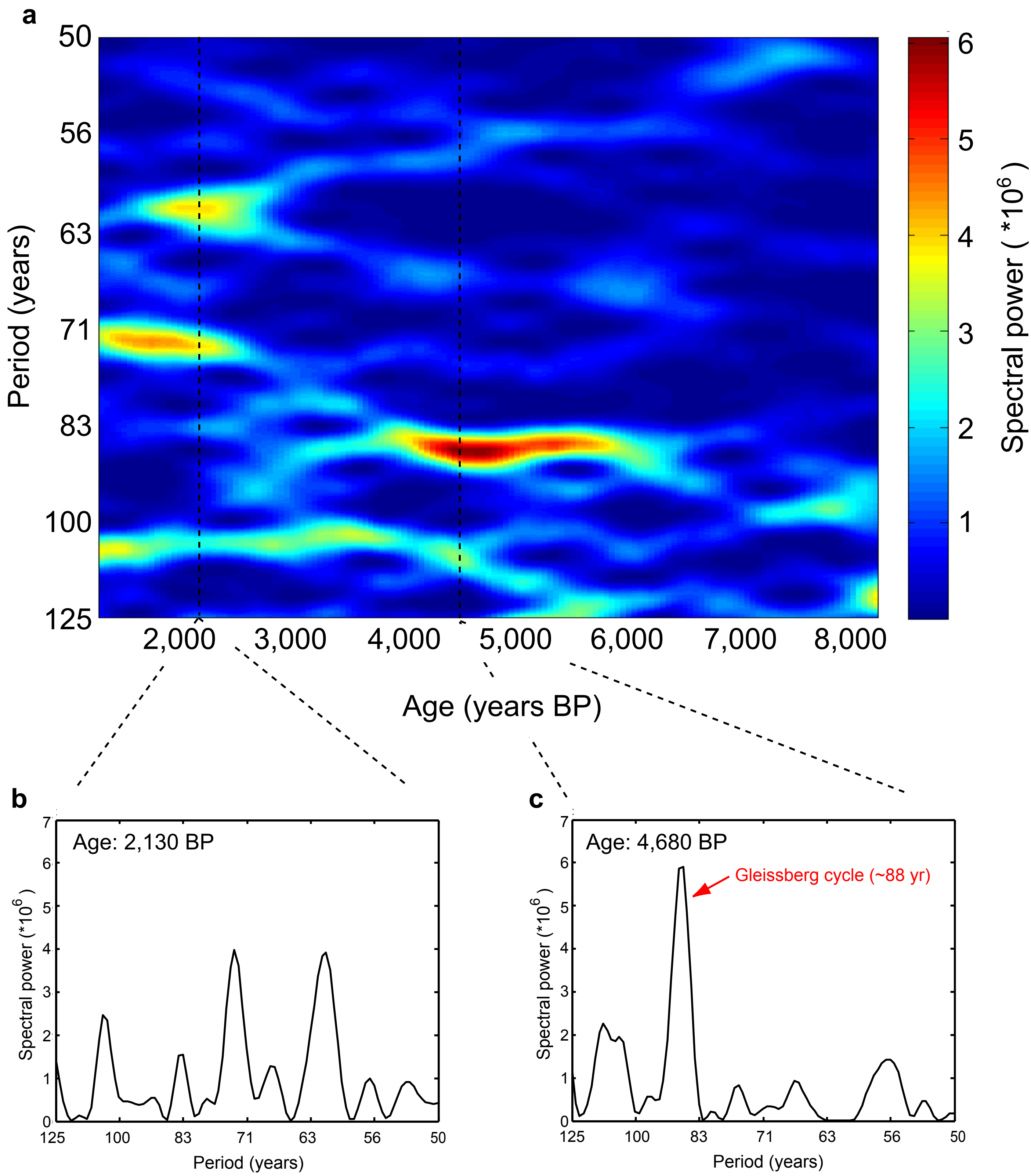

Supplementary Figure S10. Spectral density distribution of solar reconstruction based on ^{10}Be from the GRIP ice core[33]. (**a**) The spectrogram is calculated using the Lomb-Scargle fourier transform[53,54] on data grouped in 2000-yr windows, with a spacing of 50 years between each window. Note that a similar spectral density distribution is obtained if the regular fourier transform is used instead of the Lomb-Scargle fourier transform. For the solar spectrogram based on ^{10}Be, we show the distribution of spectral power, and not the spectral power exceeding the false-alarm levels, so the differences between the spectral power of various frequencies (periods) can be assessed. Moreover, other studies have already established which solar cycles are statistically significant. (**b**) An example of the spectral power distribution calculated for a 2,000-yr data window centered at 2,130 BP, and (**c**) the spectral power distribution of a 2,000-yr window centered at 4,680 BP. Notice that the Gleissberg cycle (~88 yr) is the most dominant feature in this frequency range of the ^{10}Be spectrum.

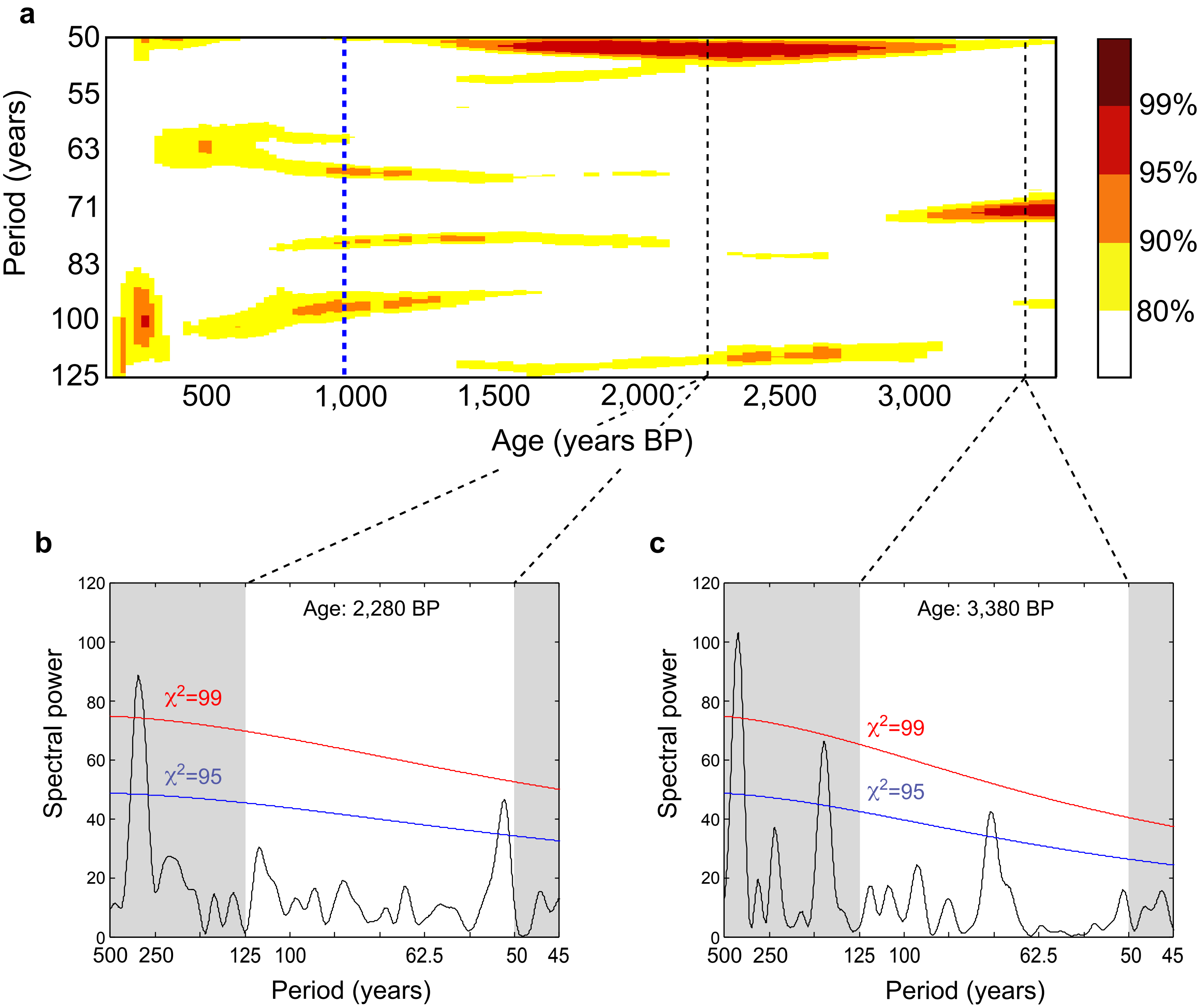

Supplementary Figure S11. Spectral density distribution of the alkenone SST record from marine core MD99-2275[50] north of Iceland. (**a**) Temporal distribution of spectral power that exceeds the red-noise false-alarm levels. The colour coding indicates that the spectral power exceeds the 80%, 90%, 95%, and 99% false-alarm levels, respectively. The spectrogram delineating the statistically significant spectral power is calculated using the Lomb-Scargle fourier transform[53,54] on data grouped in 2000-yr windows, with a spacing of 50 years between each window. However, for the interval covering the last 1,000 years (left of the dashed blue line), the size of the time window was linearly decreased from 2,000 years to 200 years in steps of 25 years. (**b**) An example of the spectral power distribution calculated for a 2,000-yr data window centered at 2,280 BP, and (**c**) the spectral power distribution of a 2,000-yr window centered at 3,380 BP. The white zones in **b** and **c** indicate the frequency interval used to construct the spectrogram in **a**. The blue and red lines in **b** and **c** denote the 95% and 99% red-noise false-alarm levels, respectively, which were calculated using the publicly available program REDFIT 3.8[31]. For the densely sampled raw data (~5 per yr) the periods shorter than ~20 yr had spectral amplitudes, which did not fit the AR1 model. We brought this record on a more equal footing with the other datasets by resampling the densely sampled raw data to double sample distance (10 yr), yielding two new "half- records". The resulting spectral periods for the two "half-records", now down to 20 yrs, did fit an AR1 process adequately for our analysis to proceed. We then calculated all spectra associated with the two new "half-records" in order to finally average the spectra and false-alarm levels associated with each time window. This approach ensured that all the data were used, and that the data complied with the red-noise model. Notice the dominant ~52-yr oscillation between 1,500 and 3,000 BP as well as the significant ~70-yr oscillation in the early part of the record.